

Autonomous Forest Inventory with Legged Robots: System Design and Field Deployment

Matias Mattamala¹, Nived Chebrolu¹, Benoit Casseau¹, Leonard Freißmuth^{1,3},
Jonas Frey^{2,4}, Turcan Tuna², Marco Hutter², Maurice Fallon¹

Abstract— We present a solution for autonomous forest inventory with a legged robotic platform. Compared to their wheeled and aerial counterparts, legged platforms offer an attractive balance of endurance and low soil impact for forest applications. In this paper, we present the complete system architecture of our forest inventory solution which includes state estimation, navigation, mission planning, and real-time tree segmentation and trait estimation. We present preliminary results for three campaigns in forests in Finland and the UK and summarize the main outcomes, lessons, and challenges. Our UK experiment at the Forest of Dean with the ANYmal D legged platform, achieved an autonomous survey of a 0.96 ha plot in 20 min, identifying over 100 trees with typical DBH accuracy of 2 cm.

I. INTRODUCTION

Systematically measuring tree attributes such as the tree height, Diameter at Breast Height (DBH), and canopy volume, is important for modern forestry [1]. This process, known as forest inventory, has traditionally involved manual tree measurement using measuring tapes and calipers and also handheld laser rangefinders [2]. Nowadays, remote sensing techniques such as Terrestrial Laser Scanning (TLS) [3] and aerial photograph [4] have massively improved the accuracy and scale at which forest inventories are built [5].

Robotics has the potential to scale this process even further. Technologies such as Simultaneous Localization And Mapping (SLAM) have been used for handheld forest mapping [6], [7]. Fixed-wing aircrafts [8] and hexacopters [9] have enabled autonomous data collection above the tree canopy where there is no risk of collision. Meanwhile small-scale drones [10], [11] and wheeled platforms [12] have been recently used for under-canopy forest inventory missions. Legged robots potentially provide significant advantages to aerial and wheeled platforms in terms of mobility, endurance, and lower soil impact [13]. However, robots have not been used for forestry tasks apart from tree harvesting [14].

In this work, we study the application of legged platforms for autonomous forest inventory tasks. Our solution combines the advanced mobility skills developed by the robotics research community [15], a robust LiDAR-based mapping system with a multi-level autonomous mission planning

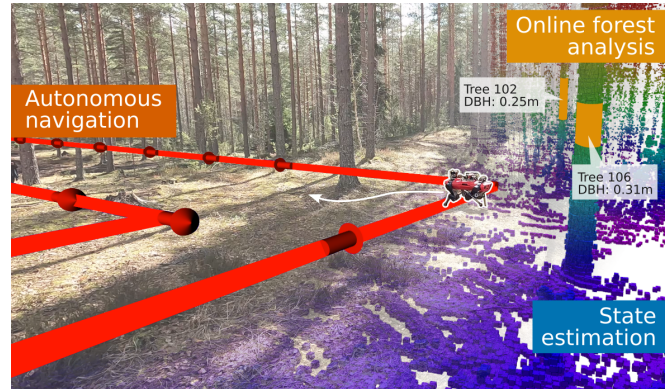


Fig. 1: We present an autonomous forest inventory solution with legged platforms. Our system aims to autonomously drive a legged platform in an unknown forest plot, while recording environmental data used for tree segmentation and trait estimation.

architecture. Our solution leverages these components to provide a consistent representation of the environment, while also enabling online processing and concurrent estimation of the forest inventory.

This paper presents ongoing work, reporting autonomous deployments executed in May 2023, October 2023, and February 2024 using our solution. Our experiments have been carried out in various forests in Finland and the UK, as shown in Fig. 1, and reflect the evolving design decisions we have made after each deployment. We discuss the findings and lessons learned, as well as the main challenges towards future autonomous forest inventory missions in the context of the DigiForest EU Horizon project¹.

II. RELATED WORK

A. Robotics-enabled forestry

Robotics has the potential to scale up forest mensuration through technologies and platforms that can automate intensive manual labor. SLAM can accelerate ground-based forest mensuration by integrating LiDAR scans from a mobile sensing payload. The produced maps can be post-processed to extract the desired attributes, such as the tree positions and DBH [6], [16], [7]. The incremental nature of SLAM and the data acquisition process has motivated the concurrent construction of maps and inventories. Chen *et al.* [10] and Proudman *et al.* [17], demonstrated real-time tree detection and DBH estimation using small-scale quadcopters and

¹The authors are with the Oxford Robotics Institute at the University of Oxford, UK. {matias, nived, benoit, mfallon}@robots.ox.ac.uk

²The authors are with the Robotic Systems Lab, ETH Zurich. {jonfrey, tutuna, mahutter}@ethz.ch

³The author is also with the Technical University of Munich, Germany. {l.freissmuth}@tum.de.

⁴The author is also with the Autonomous Learning Group, Max Planck Institute for Intelligent Systems.

¹<https://www.digiforest.eu>

handheld devices, respectively. We further explore this idea, developing an autonomy system that builds upon similar online forest inventory approaches [18].

Robotic platforms can support surveying tasks by freeing humans from collecting the data themselves [19]. In the context of aerial surveying, autonomous fixed-wing aircrafts [8], small-scale helicopters [20] and more recently hexacopter platforms [9] have been used for over-canopy data collection. As these platforms fly over the trees, most of the robotic challenges concern achieving maximum area coverage given energy [21] and time constraints [22].

Under-canopy data collection has shown more challenging, as it requires robots to operate in cluttered, unstructured spaces. For aerial platforms, this requires the use of smaller drones compared to the ones that can fly over canopy—with smaller payloads and battery size [23]. Teleoperated small-scale drones have been used for more than ten years for surveying [24], [25] though autonomous operation has been recently demonstrated for forest inventory [10], [11] and DNA sampling [26].

On the contrary, ground platforms are able to provide under-canopy measurements while carrying heavier sensing payloads, enabling longer surveys. Wheeled and tracked robot platforms have been used for forest data collection [6], [12], [27] as well as the harvesting process [28], [14], [29]. However, their larger footprint and mass contribute to soil compaction damage due to trampling [30], [31]. In this work we aim to evaluate the performance of smaller platforms—up to 50 kg.

B. Deployment of legged platforms in natural environments

The recent advances in hardware and control of legged robots makes them an compelling alternative for ground-level surveying [15].

Legged robots have been used for teleoperated soil sampling [32] as well as wildlife recording [33]. Autonomous operation in natural environments has also been demonstrated for search and rescue operations [34], load carrying tasks [35], [36], measurement of aeolian processes [37], [38], and planetary analog exploration [39].

Forestry applications have been less well unexplored, though their potential advantages (heavier payload carrying, lower soil impact) have been discussed in the past [13]. In this work, we aim to provide experimental demonstration of their capabilities for forest inventory applications.

III. AUTONOMOUS FOREST INVENTORY WITH LEGGED ROBOTS

Fig. 2 shows the system architecture of our solution, involving state estimation, legged autonomy, and forest analysis. The specific tasks and constituent modules are explained in the following sections.

A. State Estimation

Our state estimation approach involves four modules: (1) LiDAR-Inertial Odometry, (2) LiDAR SLAM, (3) dense

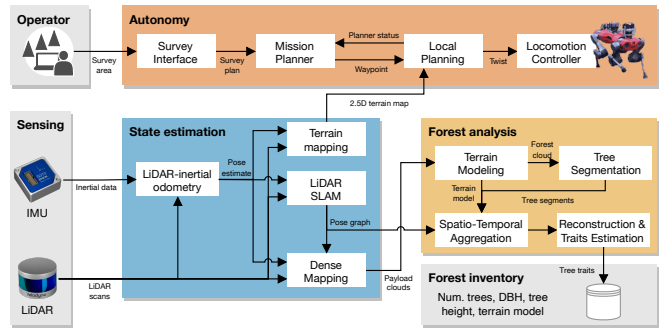


Fig. 2: System overview. The **Autonomy system** executes the mission from a survey reference given by a human operator. **State estimation** provides a consistent scene representation, as well as dense clouds which are used for tree traits estimation. **Forest analysis** segments and estimates tree traits from point cloud data. The main output of the system is a forest inventory database with the main attributes of the surveyed forest.

mapping, and (4) local terrain mapping, which provide representations for forest analysis as well as navigation.

LiDAR-Inertial Odometry: For odometry we use a LiDAR-inertial factor graph-based odometry solution, VILENS [40], which provides high-frequency pose and velocity estimates (~ 200 Hz) in a fixed inertial frame. The system performs sensor fusion of relative pose displacements from LiDAR using the Iterative Closest Point (ICP) algorithm [41] with preintegrated IMU measurements [42].

LiDAR SLAM: We use a pose graph LiDAR SLAM system [43], which incrementally builds a lightweight but consistent representation of the environment. Each graph node stores a LiDAR scan with the edge factors corresponding to incremental odometry estimates from LiDAR-Inertial odometry. We detect loop closures by checking the most recent scan against those linked to pose graph nodes within a radius of 10–15 m from the robot. The candidates are geometrically verified using ICP, and the successful candidates are added as additional factors in the pose graph. The graph is incrementally optimized using the Incremental Smoothing and Mapping (iSAM)2 algorithm [44].

Dense Mapping: As the SLAM system only stores sparse LiDAR scans within the pose graph, this map is not dense enough for further forestry analysis. We implemented a local sub-mapping module to accumulate all the incoming LiDAR scans and generate dense scans in the sensor frame, which we call *data payloads*. The data payloads are gravity-aligned and published at a slower rate (~ 0.1 Hz), accumulating clouds for about every 20 m traveled. We process these data payload to carry out online tree traits analysis (see Sec. III-C).

Local Terrain Mapping: In addition to the large-scale mapping modules, we also carry out local terrain mapping [45] and use its output in the local planner. We used a 2.5D grid-based representation with a resolution of 4 cm.

B. Autonomy System

Our autonomy system is multiple levels: spanning from the Survey Interface (Level 3) down to the low-level locomotion

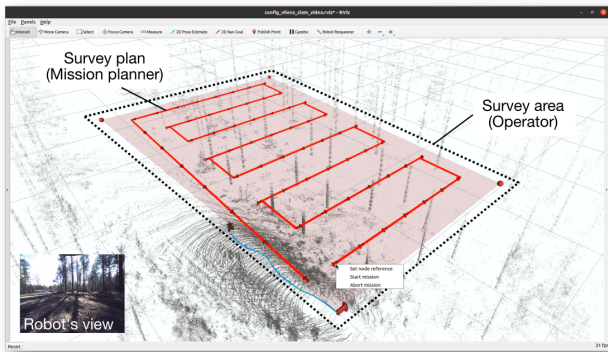


Fig. 3: Survey Interface: GUI for the operator, implemented on RViz using interactive markers. The operator defines the area to be surveyed, while the survey plan is automatically proposed by the Mission Planner.

control (Level 0).

Survey Interface (Level 3): The user interface represents the highest level of planning of our system. The human operator directly interacts to deploy the robot. We implemented it as a graphical user interface (GUI) on RViz using interactive markers. Given the initial pose of the robot, the GUI allows the operator to define a survey area and to initialize a survey plan, given by a boustrophedon decomposition, also known as lawn mower pattern [46].

The survey plan is concretely defined as a sequence of equally-spaced 6 Degrees of Freedom (DoF) waypoints, which enforce some minimum constraints to ensure that the SLAM system is able to find loop closures during operation and can keep the trajectory and the map consistent. However, this autonomy level makes no assumptions about the traversability of the surveyed area and the reachability of the waypoints, which are delegated to the lower levels of the autonomy system.

The survey interface also provides mechanisms to interrupt the mission at any time, which triggers a safe stopping behavior through the lower levels. It also enables the operator to modify and resume the plan from any specified goal.

Mission Planner (Level 2): The mission planner handles the execution of the survey plan by interacting with the local planner. In particular, it schedules the goals sent to the local planner and also processes any feedback obtained by it. For example, if the local planner reports a goal as unreachable, the mission planner chooses a new goal based on the survey plan’s state.

Local Planning (Level 1): The local planning level aims to reach the proposed goals of the plan and checks its feasibility given the state of the local environment encoded in the terrain map. A traversability estimation system first processes the local terrain map and extracts geometric features to score the terrain. The traversability score s_{trav} is specifically designed to enable navigation in the forest despite branches and twigs, though visual traversability approaches could also be used [47].

The traversability representation is used by a reactive

local planner [48], which combines different vector fields for navigation. We extended the approach to compute a Geodesic Distance Field (GDF) on a continuous cost-to-go $c_{\text{to-go}}$ obtained by the heuristic:

$$c_{\text{to-go}} = w_{\text{trav}} (1.0 - s_{\text{trav}}) + w_{\text{unkn}} s_{\text{unkn}} \quad (1)$$

where s_{unkn} is a fixed score assigned to empty cells in the terrain map (unknown), and w_{trav} , w_{unkn} are manually defined weights to leverage the contribution of the traversability score of known cells, as well as unknown ones.

The local planner measures the progress when trying to reach a waypoint, in order to detect potential situations where it is unfeasible (e.g., if the proposed waypoint is in the middle of bushes). If a goal is determined unreachable, the local planner reports this situation to the mission planner, triggering a replanning of the next goal.

Locomotion Controller (Level 0): The output of the local planner is a 3 DoF velocity command—linear (x, y), angular (yaw)—, which is executed by a low-level reinforcement learning-based locomotion controller [15]. The controller specifies a nominal walking wait for flat ground, but it relies on the local terrain map to negotiate uneven, rigid terrain. We used a pre-trained policy and did not implement any specific modifications to the architecture or training environment to operate in the forest.

C. Online Forest Analysis

Our system integrates a state estimation-driven forest inventory pipeline, presented in Freißmuth *et al.* [18]. The approach enables near real-time tree segmentation and reconstruction during the mission execution. The main steps are explained as follows, and please refer to the original work for more technical details of the implementation.

Terrain Modeling: The input to the online forest analysis step are the data payloads at 0.1 Hz. For each payload, we extract a local terrain model using the *cloth simulation filtering* method by Zhang *et al.* [49]. This enables us to segment the points belonging to the terrain from the potential tree points.

Tree Segmentation: To segment trees we use a method inspired by Cabo *et al.* [50]. We first normalize the payload cloud z-values using the terrain model, and only keep the points in a slice where we expect no tree foliage. We then use a Voronoi-based clustering to obtain tree cluster candidates. We refine the points associated to each tree by fitting a cylinder model and only keeping the points within a distance from the cylinder’s surface. The filtered tree points per tree candidates are finally de-normalized by height to obtain tree candidate clouds in the original reference frame.

Spatio-temporal Aggregation: Our system is designed to incrementally build a forest inventory, effectively improving the tree estimates and terrain model as the robot autonomously collects more data. We achieve this by exploiting the pose graph representation of the LiDAR-SLAM system, by attaching local terrain models and tree instances clouds to it, and updating them with new data after adding new poses or loop closure updates. Specifically, the global terrain

Campaign	Mission			Robot setup			Metrics					
	Date	ID	Area [m ²]	Goals	Hardware	Software	Mission time [s]	Distance traveled [m]	Area covered [ha]	Interv. [#]	MDBI [m]	MTBI [m]
Evo, Finland	2023-05-03	M1	40 × 25	Autonomy system	ANYmal C, Velodyne VLP-16	CompSLAM odometry	575.6	270.3	0.33	2	84.8	176.1
	2023-05-03	M2	40 × 25				432.4	233.6	0.32	0	233.6	432.4
	2023-05-04	M3	40 × 35				816.8*	301.1	0.37	7	30.5	72.2
	2023-05-04	M4	35 × 35				988.4	336.6	0.37	7	39.4	114.1
	2023-05-05	M5	70 × 25				1275.5	609.7	0.64	10	51.5	99.5
Wytham Woods, UK	2023-10-06	M6	20 × 20	Autonomy system, State estimation	ANYmal C, Velodyne VLP-16	VILENS odometry, VILENS-SLAM	436.9	215.0	0.29	2	69.9	136.4
Forest of Dean, UK	2023-02-19	M7	125 × 30	State estimation, Forest inventory	ANYmal D, Hesai QT64	VILENS odometry, VILENS-SLAM	1283.5	665.5	0.96	8	65.9	127.7

* This mission was manually interrupted.

TABLE I: Missions summary. We report the specifications of each mission executed across three campaigns in Finland and the UK, along with the robot setup used, as well as the main metrics reported on each mission, such as the Mean Distance Between Interventions (MDBI) and Mean Time Between Interventions (MTBI).

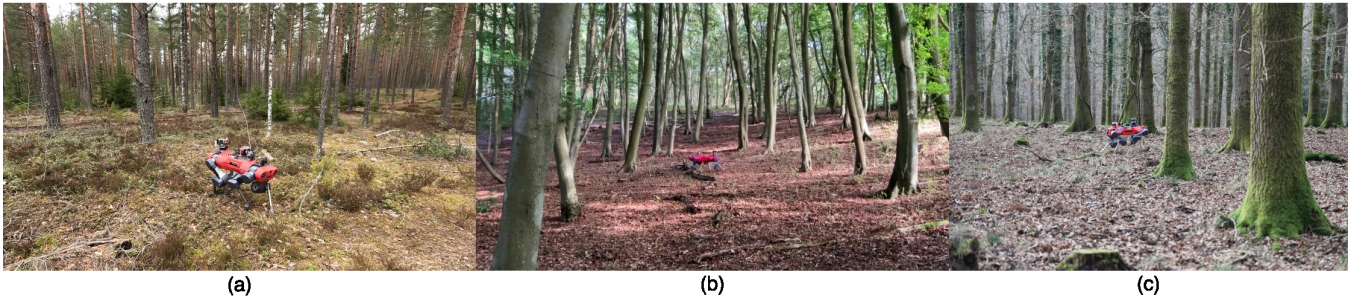


Fig. 4: Illustrative examples of the robot deployments during the different campaigns. (a) Coniferous forest in Evo, Finland. (b) Mixed forest in Wytham Woods, UK. (c) Oak forest in the Forest of Dean, UK.

model is updated by locally averaging the points around the latest terrain map using a weighted average. The tree instances clouds are managed accordingly to decide if new instances correspond to an existing tree (due to proximity) or a novel instance. We additionally check coverage conditions to ensure that high points are captured as well as even coverage from different viewpoints.

Tree Reconstruction and Trait Estimation: Lastly, we estimate the traits required by the forest inventory. Particularly, we first aim to *reconstruct* the tree by fitting circles along the stem, and then reconstructing the trunk as a collection of oblique cone frustums. The reconstructions are then used to recover geometric traits such as the DBH and tree height. The traits are reported to the operator and also exported as a *marteloscope*—a 2D representation of the forest.

IV. EXPERIMENTS

A. Campaign description

We executed three field campaigns in different forests in Finland and the UK, which are summarized in Tab. I. Five missions (M1-M5) were executed in conifer forests in Evo, Finland in May 2023. The other two were ran in the UK, in mixed (M6, at Wytham Woods, in October 2023) and oak forests (M7, at the Forest of Dean, in February 2024). While

the two former had the objective of testing the autonomy system, the latter also focused on the online forest analysis integration. Fig. 4 illustrates some examples of the robot deployed in the field.

B. Deployment methodology

All the missions followed the same procedure. A *robot operator* was in charge of defining the survey mission and supervising the overall execution. A *safety operator*, carrying a remote controller to overrule the autonomy system, followed the robot at a safe distance during the mission to avoid undesired situations (e.g. collisions and *cul-de-sacs*).

We logged all the signals from the robot and the autonomy system, as well as the actions executed by the safety operator. The safety interventions were the main signal we used for evaluating the performance of the autonomy system, as it enables the use of metrics such as the Mean Distance Between Interventions (MDBI) and MTBI, as done in autonomous driving literature [51]. However, instead of computing the metrics using the total distance traveled over the number of interventions reported, we determined the average by measuring the actual time and distance intervals when the robot was effectively walking autonomously. We call these measurements *autonomy segments*, shown in blue in the

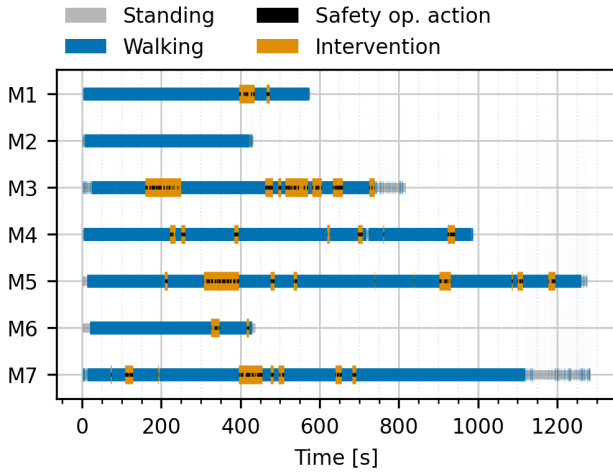


Fig. 5: Summary of the seven survey missions executed across the three campaigns. We illustrate the periods where the robots operated fully autonomously, and where they required manual interventions from the safety operator.

summary plot (Fig. 5).

C. Evo Campaign

Our first campaign, in Finland, had the goal of evaluating the proposed autonomy system in forest environments. This was executed with an ANYmal C platform, using the Velodyne VLP-16 (30° Field-of-View (FoV)) as the main environmental sensor. We used a state estimation setup derived from the CERBERUS SubT stack [52], which used CompSLAM [53] as the main odometry system. CompSLAM does not perform online pose graph optimization and loop-closure detection to ensure consistency.

Fig. 5 shows the autonomy performance reported in these missions (M1-M5), while Fig. 4 (a) shows an example from M2. Missions M1 and M2 were executed in the same plots, obtaining consistent results. Mission M3 was executed in an area nearby, but with more challenging terrain, which required to interrupt the mission due to the robot getting trapped in a damp area (Fig. 6). Missions M4 and M5 were executed in different areas of the forest, but achieving similar area coverage per time unit (1.5 ha), as shown in Tab. I. In M5, we additionally observed severe tracking problems with the reference survey path due to drift in the state estimation system, which were more evident in this longer sequence (600 m long, compared to 300 m set for the other missions).

The missions lasted between 10–20 min, with the robot walking up to 600 m on the longest missions. About the autonomy performance, while we report the MDBI and MTBI in Tab. I, we found the fine grained analysis of the distribution of autonomy segments a more informative metric. This is shown in Fig. 7. With exception of mission M2, which was fully autonomous, in most of the other missions we reported a higher density of short autonomy segments (~ 10 m or ~ 50 s). Many cases were due to short, frequent ‘pushes’ performed by the safety operator to move



Fig. 6: Failure case in mission M3 in Evo, Finland. The robot was trapped due to damp terrain, which was not detected by the onboard perception systems.

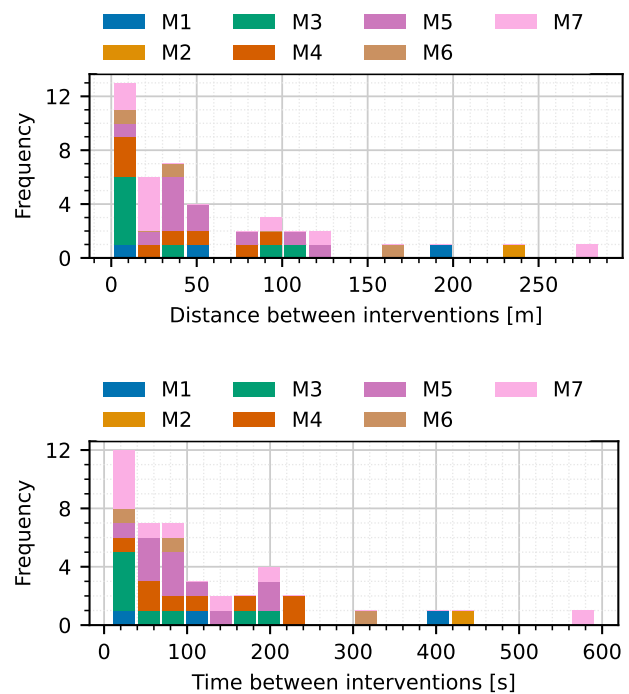


Fig. 7: Distribution of distance and time between interventions for all missions. *Top*: Distance between interventions. *Bottom*: Time between interventions.

the local planner solution out of local minima, or driving the robot around a dead end.

We additionally reported how long the interventions took on each mission (Fig. 8). We observed that most of the interventions were ~ 15 s, which is within the time required for the safety operator to get the robot out of dead ends that the mission and local planner interaction was not able to solve automatically. Only in specific cases—M3 and M5—, where the robot was deployed in considerably more challenging environments (damp terrain, short trees, higher density of bushes) we required longer interventions (>1 min) to move the robot to safer areas before continuing the mission.

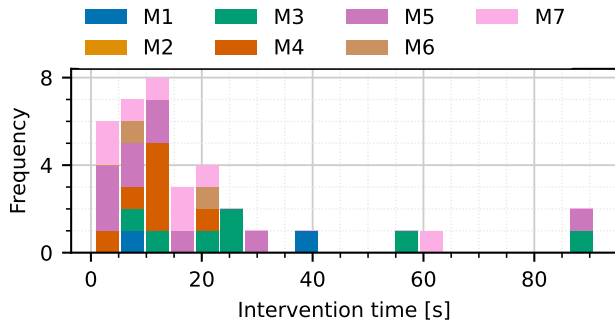


Fig. 8: Duration of the interventions reported for each mission. Most of the interventions reported were short—20 s on average.

D. Wytham Woods Campaign

The second campaign was executed in the UK, in a mixed forest plot in Wytham Woods, near Oxford. The same ANYmal C platform and LiDAR setup was used in this campaign, as the goal was to improve the state estimation solution problems reported in the Evo campaign. For this, we transitioned to the proposed state estimation solution, which explicitly relied on a LiDAR-inertial odometry system along with an online pose graph SLAM to ensure consistency.

Fig. 4 (b) shows the testing environment, which was a clear sloped plot, with a few loose branches and twigs. We set a smaller $20\text{ m} \times 20\text{ m}$ survey area, which corresponded to 0.29 ha covered for an effective 15 m LiDAR range. The reported coverage rate was consistent with the results obtained in the Evo campaign, above 1.5 ha/h . Only two short interventions were required (see Fig. 8, M6) to avoid falls due to loose branches, which trapped the robot’s legs.

E. Forest of Dean Campaign

The last campaign, executed in the Forest of Dean in the UK, was used to test the integration of the forest analysis system towards online forest inventory. Additionally, we changed the robot platform from ANYmal C to ANYmal D—which has longer shanks, though the locomotion policy does not exploit this fact explicitly. We also improved the sensor payload, where we used a sensing unit with a dedicated computer and a Hesai QT64 LiDAR, which as a larger vertical FoV (104°), enabling better coverage of the full trees. The state estimation and autonomy were left unchanged apart from the sensor configuration, as they were validated in the previous campaigns.

For the specific mission we executed, denoted M7, we specified a $125\text{ m} \times 30\text{ m}$ survey area, which effectively corresponded to a 0.96 ha plot. The robot completed the mission in approximately 20 min, segmenting up to 100 trees, as shown in Fig. 9. Fig. 10 shows the marteloscope, which summarizes the tree positions and DBH reported for the trees successfully reconstructed by our proposed online forest analysis pipeline.

V. CURRENT CHALLENGES AND FUTURE WORK

Our deployments so far have allowed us to continuously refine and improve our proposed forest inventory solution, from a software and hardware perspective. Our experiments to date indicate that, given the robot capabilities and the sensing setup, our solution should enable the autonomous inventory at 2 ha/h . This is a feasible bound given the battery specifications of the ANYmal platform, assuming fairly clean forest areas without challenging ground vegetation. Nevertheless, we still observe open challenges to address to improve the performance of our systems towards autonomous inventory and monitoring.

Autonomy performance: Firstly, we aim to improve the performance reported through the MDBI and MTBI metrics. Across the missions we did not observe a clear trend of improvement, partly caused by the changes in the constituent components but also due to measuring the metrics in completely different environments. To improve performance, we identified potential improvements in the autonomy system. Particularly by designing new re-planning strategies to detect and navigate around untraversable areas effectively, identifying and avoiding dead ends, as well as maximizing loop closure corrections.

Locomotion and navigation: In spite of using a robust locomotion controller, we observed that further improvements are still required to negotiate branches and twigs in a safer manner, to avoid potential falls and failures due to trapped legs. This could be solved by low-level strategies to vary the step size, or by identifying such areas with the onboard perception systems, effectively guiding the robot through longer-though-safer paths.

Forestry tasks integration: Lastly, we identified further improvements can be achieved for the real-world usability of our solution. Practical issues such as improving long-range communication in the forest, could enable better feedback of the operation, and provide live reporting of the estimated traits for the foresters. Additionally, studying the impact of legged locomotion on the forest soil, as well as practical comparisons to alternative inventory approaches could further contribute to the adoption of these platforms for forestry.

VI. CONCLUSION

In this work, we presented ongoing efforts to develop an autonomous forest inventory system with small-scale legged platforms. Through seven different missions in forests in Finland and the UK, we have demonstrated the feasibility of using legged platforms for these tasks, providing a systematic way to survey and study natural environments. We have also presented open challenges, which we identified during our deployments. While some of them will be improved for future field deployments, they also present research questions that can be of interest to the field and legged robotics communities.

VII. ACKNOWLEDGMENTS

This work is supported by EU Horizon 2020 (101070405 DigiForest) as well as a Royal Society University Research

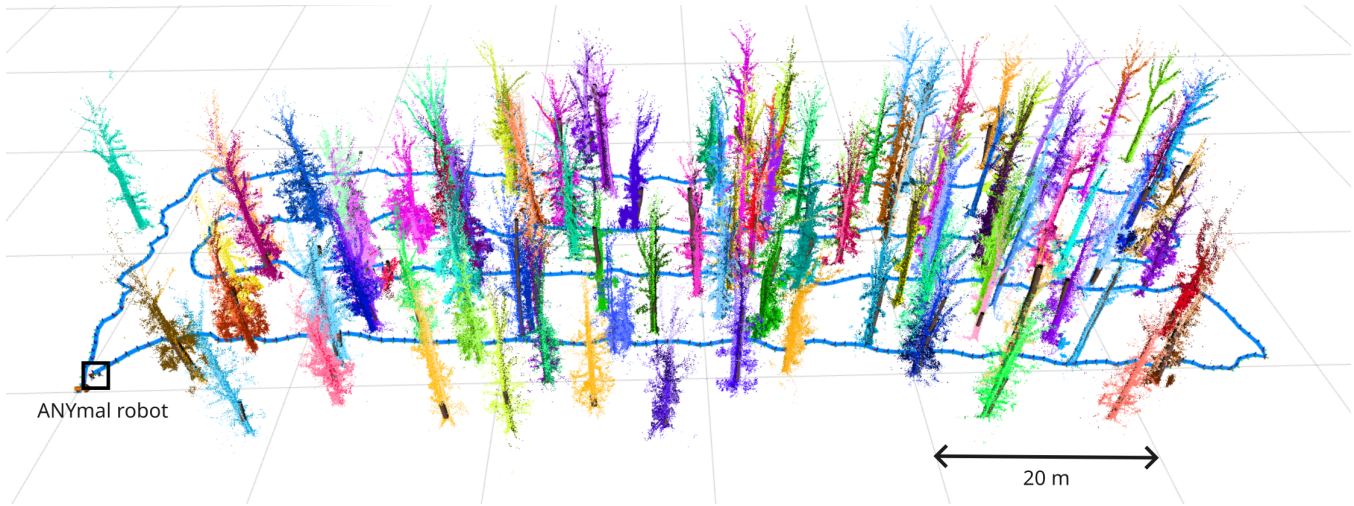


Fig. 9: Illustrative example of the output produced by our system after an autonomous mission in the Forest of Dean, UK. The robot surveyed 0.96 ha in 20 min, and around 100 trees were segmented during online operation.

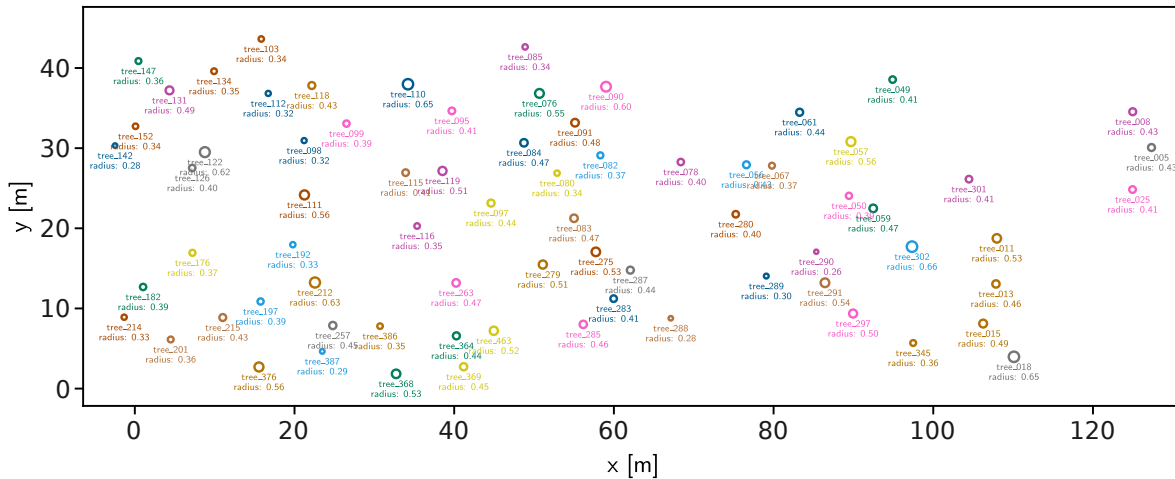


Fig. 10: Marteloscope produced after the deployment in the forest of Dean, indicating the tree positions and the DBH of the successfully reconstructed trees.

Fellowship. We acknowledge PreFor Oy for organizing the Evo campaign, as well as Forest Research UK for arranging the Forest of Dean campaign.

REFERENCES

- [1] C. L. Brack, "Forest measurement and modeling - measuring trees, stands and forests for effective forest management," Australian National University, Tech. Rep., 2001. [Online]. Available: <http://fennerschool-associated.anu.edu.au/mensuration/index.htm>
- [2] G. J. Hamilton, *Forest mensuration handbook*. Forestry Commission, 1988.
- [3] R. O. Dubayah and J. B. Drake, "Lidar Remote Sensing for Forestry," *Journal of Forestry*, vol. 98, no. 6, pp. 44–46, June 2000.
- [4] R. J. Hall, "The Roles of Aerial Photographs in Forestry Remote Sensing Image Analysis," in *Remote Sensing of Forest Environments: Concepts and Case Studies*, M. A. Wulder and S. E. Franklin, Eds. Boston, MA: Springer US, 2003, pp. 47–75.
- [5] X. Liang, V. Kankare, J. Hyypää, Y. Wang, A. Kukko, H. Haggrén, X. Yu, H. Kaartinen, A. Jaakkola, F. Guan, M. Holopainen, and M. Vastaranta, "Terrestrial laser scanning in forest inventories," *ISPRS J. Photogramm. Remote Sens.*, vol. 115, pp. 63–77, 2016.
- [6] M. Miettinen, M. Ohman, A. Visala, and P. Forsman, "Simultaneous localization and mapping for forest harvesters," in *IEEE Int. Conf. Robot. Autom.*, 2007, pp. 517–522.
- [7] J.-F. Tremblay, M. Béland, R. Gagnon, F. Pomerleau, and P. Giguère, "Automatic three-dimensional mapping for tree diameter measurements in inventory operations," *J. Field Robot.*, vol. 37, no. 8, pp. 1328–1346, 2020.
- [8] L. P. Koh and S. A. Wich, "Dawn of Drone Ecology: Low-Cost Autonomous Aerial Vehicles for Conservation," *Tropical Conservation Science*, vol. 5, no. 2, pp. 121–132, June 2012.
- [9] D. R. A. Almeida, A. M. Almeyda Zambrano, E. N. Broadbent, A. L. Wendt, P. Foster, B. E. Wilkinson, C. Salk, D. D. A. Papa, S. C. Stark, R. Valbuena, E. B. Gorgens, C. A. Silva, P. H. S. Brancalion, M. Fagan, P. Meli, and R. Chazdon, "Detecting successional changes in tropical forest structure using GatorEye drone-borne lidar," *Biotropica*, vol. 52, no. 6, pp. 1155–1167, Nov. 2020.
- [10] S. W. Chen, G. V. Nardari, E. S. Lee, C. Qu, X. Liu, R. A. F. Romero, and V. Kumar, "Sloam: Semantic lidar odometry and mapping for forest inventory," *IEEE Robot. Autom. Lett.*, vol. 5, no. 2, pp. 612–619, 2020.
- [11] X. Liu, G. V. Nardari, F. C. Ojeda, Y. Tao, A. Zhou, T. Donnelly, C. Qu, S. W. Chen, R. A. F. Romero, C. J. Taylor, and V. Kumar, "Large-scale autonomous flight with real-time semantic slam under dense forest canopy," *IEEE Robot. Autom. Lett.*, vol. 7, no. 2, pp. 5512–5519, 2022.

- [12] M. Pierzchała, P. Giguère, and R. Astrup, "Mapping forests using an unmanned ground vehicle with 3D LiDAR and graph-SLAM," *Comput. Electron. Agr.*, vol. 145, pp. 217–225, Feb. 2018.
- [13] D. J. Todd, *Applications of walking machines*. Boston, MA: Springer US, 1985, pp. 169–177.
- [14] E. Jelavic, D. Jud, P. Egli, and M. Hutter, "Robotic precision harvesting: Mapping, localization, planning and control for a legged tree harvester," *Field Robotics*, 2021.
- [15] T. Miki, J. Lee, J. Hwangbo, L. Wellhausen, V. Koltun, and M. Hutter, "Learning robust perceptive locomotion for quadrupedal robots in the wild," *Sci. Robot.*, vol. 7, no. 62, 2022.
- [16] J. Tang, Y. Chen, A. Kukko, H. Kaartinen, A. Jaakkola, E. Khoramshahi, T. Hakala, J. Hyypää, M. Holopainen, and H. Hyypää, "SLAM-Aided Stem Mapping for Forest Inventory with Small-Footprint Mobile LiDAR," *Forests*, vol. 6, no. 12, pp. 4588–4606, Dec. 2015.
- [17] A. Proudman, M. Ramezani, S. T. Digumarti, N. Chebrolu, and M. Fallon, "Towards real-time forest inventory using handheld lidar," *Robotics and Autonomous Systems*, vol. 157, p. 104240, 2022.
- [18] L. Freißmuth, M. Mattamala, N. Chebrolu, S. Schaefer, S. Leutenegger, and M. Fallon, "Online Tree Reconstruction and Forest Inventory on a Mobile Robotic System," 2024, (Under review).
- [19] K. Anderson and K. J. Gaston, "Lightweight unmanned aerial vehicles will revolutionize spatial ecology," *Frontiers in Ecology and the Environment*, vol. 11, no. 3, pp. 138–146, 2013.
- [20] J. R. Kellner, J. Armston, M. Birrer, K. C. Cushman, L. Duncanson, C. Eck, C. Fallegger, B. Imbach, K. Král, M. Krůček, J. Trochta, T. Vrška, and C. Zraggen, "New Opportunities for Forest Remote Sensing Through Ultra-High-Density Drone Lidar," *Surveys in Geophysics*, vol. 40, no. 4, pp. 959–977, July 2019.
- [21] K. Shah, G. Ballard, A. Schmidt, and M. Schwager, "Multidrone aerial surveys of penguin colonies in antarctica," *Sci. Robot.*, vol. 5, no. 47, p. eabc3000, 2020.
- [22] D. C. Schedl, I. Kurmi, and O. Bimber, "An autonomous drone for search and rescue in forests using airborne optical sectioning," *Sci. Robot.*, vol. 6, no. 55, p. eabg1188, 2021.
- [23] X. Zhou, X. Wen, Z. Wang, Y. Gao, H. Li, Q. Wang, T. Yang, H. Lu, Y. Cao, C. Xu, and F. Gao, "Swarm of micro flying robots in the wild," *Sci. Robot.*, vol. 7, no. 66, p. eabm5954, 2022.
- [24] Y. Lin, J. Hyypää, and A. Jaakkola, "Mini-UAV-Borne LiDAR for Fine-Scale Mapping," *IEEE Geosci. Remote Sens. Lett.*, vol. 8, no. 3, pp. 426–430, May 2011.
- [25] E. Hyypää, J. Hyypää, T. Hakala, A. Kukko, M. A. Wulder, J. C. White, J. Pyörälä, X. Yu, Y. Wang, J.-P. Virtanen, O. Pohjavirta, X. Liang, M. Holopainen, and H. Kaartinen, "Under-canopy UAV laser scanning for accurate forest field measurements," *ISPRS J. Photogramm. Remote Sens.*, vol. 164, pp. 41–60, June 2020.
- [26] E. Aucone, S. Kirchgeorg, A. Valentini, L. Pellissier, K. Deiner, and S. Mintchev, "Drone-assisted collection of environmental DNA from tree branches for biodiversity monitoring," *Sci. Robot.*, vol. 8, no. 74, p. eadd5762, 2023.
- [27] A. Tominaga, H. Eiji, and A. Mowshowitz, "Development of Navigation System in Field Robot for Forest Management," in *Int. Conf. Soft Comput. Intell. Syst. and Int. Sym. Adv. Intell. Syst.*, Toyama, Japan, Dec. 2018, pp. 1142–1147.
- [28] J. Rossmann, M. Schluse, C. Schlette, A. Buecken, P. Krahwinkler, and M. Emde, "Realization of a highly accurate mobile robot system for multi purpose precision forestry applications," in *2009 International Conference on Advanced Robotics*, June 2009, pp. 1–6.
- [29] E. Jelavic, T. Kapgen, S. Kerscher, D. Jud, and M. Hutter, "Harveri : A Small (Semi-)Autonomous Precision Tree Harvester," in *Innovation in Forestry Robotics: Research and Industry Adoption (ICRA 2022)*, May 2022.
- [30] S. Fountas, T. A. Gemtos, and S. Blackmore, *Robotics and Sustainability in Soil Engineering*. Berlin, Heidelberg: Springer Berlin Heidelberg, 2010, pp. 69–80.
- [31] A. Calleja-Huerta, M. Lamandé, O. Green, and L. Munkholm, "Vertical and horizontal stresses from a lightweight autonomous field robot during repeated wheeling," *Soil and Tillage Research*, vol. 233, p. 105790, Sept. 2023.
- [32] C. G. Wilson, F. Qian, D. J. Jerolmack, S. Roberts, J. Ham, D. Koditschek, and T. F. Shipley, "Spatially and temporally distributed data foraging decisions in disciplinary field science," *Cognitive Research: Principles and Implications*, vol. 6, no. 1, p. 29, 2021.
- [33] K. Melo, T. Horvat, and A. J. Ijspeert, "Animal robots in the african wilderness: Lessons learned and outlook for field robotics," *Sci. Robot.*, vol. 8, no. 85, p. eadd8662, 2023.
- [34] M. Tranzatto, M. Dharmadhikari, L. Bernreiter, M. Camurri, S. Khatkhat, F. Mascarich, P. Pfreundschuh, D. Wisth, S. Zimmermann, M. Kulkarni, V. Reijgwart, B. Casseau, T. Homberger, P. D. Petris, L. Ott, W. Tubby, G. Waibel, H. Nguyen, C. Cadena, R. Buchanan, L. Wellhausen, N. Khedekar, O. Andersson, L. Zhang, T. Miki, T. Dang, M. Mattamala, M. Montenegro, K. Meyer, X. Wu, A. Briod, M. Mueller, M. Fallon, R. Siegwart, M. Hutter, and K. Alexis, "Team CERBERUS Wins the DARPA Subterranean Challenge: Technical Overview and Lessons Learned," 2022.
- [35] D. Wooden, M. Malchano, K. Blankespoor, A. Howard, A. A. Rizzi, and M. H. Raibert, "Autonomous navigation for bigdog," in *IEEE Int. Conf. Robot. Autom.*, 2010, pp. 4736–4741.
- [36] D. M. Bradley, J. K. Chang, D. Silver, M. Powers, H. Herman, P. Rander, and A. Stentz, "Scene understanding for a high-mobility walking robot," in *IEEE/RSJ Int. Conf. Intell. Robots Syst.*, 2015, pp. 1144–1151.
- [37] F. Qian, D. Jerolmack, N. Lancaster, G. Nikolich, P. Reverdy, S. Roberts, T. Shipley, R. S. Van Pelt, T. M. Zobeck, and D. E. Koditschek, "Ground robotic measurement of aeolian processes," *Aeolian Research*, vol. 27, pp. 1–11, 2017.
- [38] F. Qian, D. Lee, G. Nikolich, D. Koditschek, and D. Jerolmack, "Rapid in situ characterization of soil erodibility with a field deployable robot," *Journal of Geophysical Research: Earth Surface*, vol. 124, no. 5, pp. 1261–1280, 2019.
- [39] P. Arm, G. Waibel, J. Preisig, T. Tuna, R. Zhou, V. Bickel, G. Ligeza, T. Miki, F. Kehl, H. Kolvenbach, and M. Hutter, "Scientific exploration of challenging planetary analog environments with a team of legged robots," *Sci. Robot.*, vol. 8, no. 80, p. eade9548, 2023.
- [40] D. Wisth, M. Camurri, and M. Fallon, "Vilens: Visual, inertial, lidar, and leg odometry for all-terrain legged robots," *IEEE Trans. Robot.*, vol. 39, no. 1, pp. 309–326, 2023.
- [41] P. J. Besl and N. D. McKay, "A method for registration of 3-d shapes," *IEEE Trans. Pattern Anal. Mach. Intell.*, vol. 14, no. 2, pp. 239–256, 1992.
- [42] C. Forster, L. Carlone, F. Dellaert, and D. Scaramuzza, "On-manifold preintegration for real-time visual-inertial odometry," *IEEE Trans. Robot.*, vol. 33, no. 1, pp. 1–21, 2017.
- [43] M. Ramezani, G. Tinchev, E. Iuganov, and M. Fallon, "Online LiDAR-SLAM for Legged Robots with Robust Registration and Deep-Learned Loop Closure," in *IEEE Int. Conf. Robot. Autom.*, 2020, pp. 4158–4164.
- [44] M. Kaess, H. Johannsson, R. Roberts, V. Ila, J. J. Leonard, and F. Dellaert, "iSAM2: Incremental smoothing and mapping using the Bayes tree," *Int. J. Robot. Res.*, vol. 31, no. 2, pp. 216–235, 2012.
- [45] P. Fankhauser, M. Bloesch, and M. Hutter, "Probabilistic terrain mapping for mobile robots with uncertain localization," *IEEE Robot. Autom. Lett.*, vol. 3, no. 4, pp. 3019–3026, 2018.
- [46] H. Choset, "Coverage of known spaces: The boustrophedon cellular decomposition," *Auton. Robots*, vol. 9, no. 3, pp. 247–253, 2000.
- [47] J. Frey, M. Mattamala, N. Chebrolu, C. Cadena, M. Fallon, and M. Hutter, "Fast Traversability Estimation for Wild Visual Navigation," in *Robot.: Sci. Syst.*, 2023.
- [48] M. Mattamala, N. Chebrolu, and M. F. Fallon, "An efficient locally reactive controller for safe navigation in visual teach and repeat missions," *IEEE Robot. Autom. Lett.*, vol. 7, no. 2, pp. 2353–2360, 2022.
- [49] W. Zhang, J. Qi, P. Wan, H. Wang, D. Xie, X. Wang, and G. Yan, "An easy-to-use airborne lidar data filtering method based on cloth simulation," *Remote Sens.*, vol. 8, no. 6, p. 501, 2016.
- [50] C. Cabo, C. Ordóñez, C. A. López-Sánchez, and J. Armesto, "Automatic dendrometry: Tree detection, tree height and diameter estimation using terrestrial laser scanning," *Int. J. Appl. Earth Obs. Geoinformation*, vol. 69, pp. 164–174, 2018.
- [51] D. Paz, P. Lai, N. Chan, Y. Jiang, and H. I. Christensen, "Autonomous vehicle benchmarking using unbiased metrics," in *IEEE/RSJ Int. Conf. Intell. Robots Syst.*, 2020, pp. 6223–6228.
- [52] M. Tranzatto, T. Miki, M. Dharmadhikari, L. Bernreiter, M. Kulkarni, F. Mascarich, O. Andersson, S. Khattak, M. Hutter, R. Siegwart, and K. Alexis, "CERBERUS in the DARPA subterranean challenge," *Sci. Robot.*, vol. 7, no. 66, 2022.
- [53] S. Khattak, H. Nguyen, F. Mascarich, T. Dang, and K. Alexis, "Complementary multi-modal sensor fusion for resilient robot pose estimation in subterranean environments," in *Int. Conf. on Unmanned Aircraft Systems (ICUAS)*, 2020, pp. 1024–1029.